CSIRO Publishing

Publications of the Astronomical Society of Australia

VOLUME 18, 2001

An international journal of astronomy and astrophysics

For editorial enquiries and manuscripts, please contact:
The Editor, PASA,
ATNF, CSIRO,
PO Box 76,
Epping, NSW 1710, Australia
Telephone: +61 2 9372 4590
Fax: +61 2 9372 4310
Email: Michelle.Storey@atnf.csiro.au

For general enquiries and subscriptions, please contact:
CSIRO Publishing
PO Box 1139 (150 Oxford St)
Collingwood, Vic. 3066, Australia
Telephone: +61 3 9662 7666
Fax: +61 3 9662 7555
Email: pasa@publish.csiro.au

Published by CSIRO Publishing
for the Astronomical Society of Australia

www.publish.csiro.au/journals/pasa

https://doi.org/10.1071/AS01014 Published online by Cambridge University Press

Publ. Astron. Soc. Aust., 2001, 18, 211–214

Source Size Measurement from Observed Quasar Microlensing

Atsunori Yonehara*

Department of Astronomy, Kyoto University, Sakyo-ku, Kyoto, 606-8502, Japan
*Research Fellow of the Japan Society for the Promotion of Science

Received 2001 January 21, accepted 2001 May 5

Abstract: Recently, the OGLE team have reported a clear quasar microlensing signal in Q2237+0305. I have analyzed the microlens event of 'image C' by using their finely and densely sampled light curves. From light curve fitting, I unambiguously set the source size of $\leq$0.98 Einstein-Ring radius as a conservative limit. This limit corresponds to 2000 AU, if I adopt $M_{lens} \sim 0.1 M_{\odot}$ obtained by a recent statistical study of the mean mass of the lens object. This gives clear evidence for the existence of an accretion disk in the central region of the quasar.

Keywords: accretion, accretion disks — galaxies: active — gravitational lensing — quasars: individual (Q2237+0305)

1 Introduction

Since the discovery of quasars, one of the attractive subjects in astronomy/astrophysics is to reveal their structure. Currently, previous observational and theoretical studies strongly suggest the existence of an accretion disk in the innermost region of quasars. The apparent size of the accretion disk is estimated to be $\sim$1 μarcsec. Unfortunately, due to such small apparent angular size, it is impossible to resolve the accretion disk directly. Thus, we do not have any direct evidence for the existence of the accretion disk.

However, there is a fascinating way to get rid of such difficulties — the diagnosis method by using 'quasar microlensing'. Applicable targets for such a technique are limited (e.g. Q2237+0305), but surprisingly, the spatial resolution of the technique ($\leq$1 μarcsec) reaches far below that of current observational instruments. Thus, we can probe the innermost region of quasars via microlensing (e.g., see Wambsganss 2001; Mineshige, Yonehara & Takahashi 2001).

Recently, the OGLE group has reported new evident signals of quasar microlensing in Q2237+0305 (so-called 'Huchra's lens' or 'Einstein Cross', see Wozniak et al. 2000). Here, I present an analysis of the quasar microlensing light curve of image C (see also Shalyapin 2001).

In Section 2, I briefly explain the method of light curve fitting, and the results and discussions are presented in Section 3.

2 Method

First of all, I have to know about the magnification pattern to obtain ideal light curves of quasar microlensing. Generally, in the case of quasar microlensing, the magnification patterns are complicated and hugely varied (e.g., Wambsganss, Schneider & Pazcyński 1990). In contrast, if the mass fraction of the objects that contribute to the microlensing events is small ($\sim$10%), there is a typical magnification pattern. The magnification pattern in the case of small mass fraction is almost identical to that of the Chang & Refsdal (1984) lens case. In Figure 1, examples

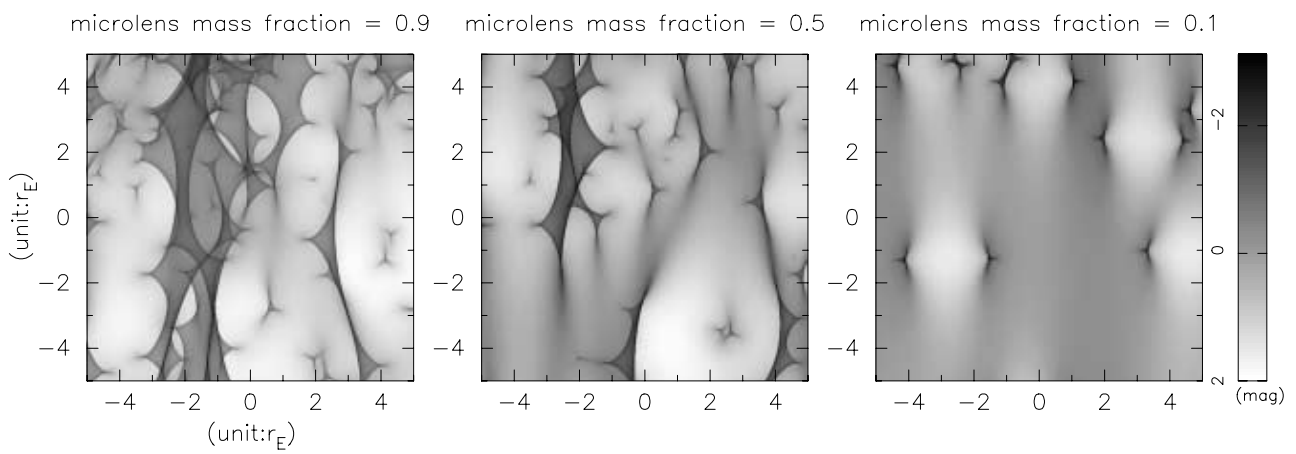

Figure 1 Magnification patterns for quasar microlensing in the case of microlens mass fraction = 0.9, 0.5, and 0.1 are displayed in left, middle, and right panel, respectively. These figures are calculated from the code developed by Wambsganss (1990).

 10.1071/AS01014 1323-3580/01/020211$05.00

of magnification patterns for quasar microlensing on the image C are presented. Then, I assume such a situation and apply the convergence (κ) and shear (γ) value on the image C which was obtained by Schmidt, Webster & Lewis (1998), i.e. $\kappa = 0.69$ and $\gamma = 0.71$.

Even if I accept such simplification, it will be difficult to calculate the exact magnification factor in the case of finite-size sources. Thus, I adopt approximated formulae for the magnification factor in the vicinity of fold (Fluke & Webster 1999) and cusp caustics (Zakharov 1995). Both of these two sorts of caustics seem to induce the observed, highly magnified microlensing event in image C. Furthermore, in the case of the Chang & Refsdal (1984) lens, two different types of cusp caustics and several fold caustics can be formed. Then, I consider two distinctive cusp caustics cases and four representative fold caustics cases for magnification, numerically integrate the magnification factor over the source, and obtain the effective magnification factor for the circular, finite-size, uniform brightness source with a given radius (normalised by the Einstein-Ring radius, $r_{\rm E}$).

Finally, to get the best-fit light curve and a corresponding set of parameters, I employ the standard method, i.e., the minimization of the χ^2 value between the observed light curve (number of data points = 83) and an ideal light curve for a given set of parameters. The set of parameters consists of source size, velocity relative to the caustic, impact parameter, the epoch of caustic crossing, constant magnification and its gradual change caused by other caustics. The total number of parameters to calculate the light curve are 6 and 7 for the fold and the cusp caustics cases, respectively. The adopted method to minimize the χ^2 value is a kind of downhill simplex method, so-called AMOEBA (Press et al. 1992). After obtaining the set of best-fit parameters, I have also estimated the confidence region for parameters by using a Monte Carlo method as follows. (1) By supposing that the best-fit parameter is a real parameter, I calculate an ideal light curve without any errors. (2) By adding random errors to the magnitude corresponding to the observational error dispersion and by sampling this light curve at the times corresponding to the actually observed times, I obtain a mock light curve. (3) By using this mock light curve, I again perform a light curve fitting and obtain a set of the best-fit parameters for the mock light curve. (4) By iterating procedures (2) and (3) many times, in this study 100 times, and summarising the best-fit values for the mock light curves, I can evaluate the confidence region.

Details about the above procedures are shown in Yonehara (2001).

3 Results and Discussions

The resultant, best-fit light curves are shown in Figure 2 and corresponding paths of the source relative to the caustic are also shown in Figure 3. Evidently, the best-fit parameters finely reproduce the observed light curves. The resultant source size and the reduced χ^2 ($\bar{\chi}^2$) are presented in Table 1. In this table the estimated confidence regions are also presented.

In the case of an infinitely small-size source (a point source), the expected microlens light curves are quite different from case to case, e.g. light curves for the fold caustics case and those for the cusp caustics cases are clearly different. Moreover, in the case of a caustic crossing event, the light curve should show a spiky feature around its peak flux and, hence, such a case can be safely rejected (see Figure 4). Conversely, if the finite-size source effect is taken into account, such a spiky peak will be smeared out and I can manage to reproduce the observed light curve with an acceptable goodness of fit ($\bar{\chi}^2 \sim 1$) as you can see in Table 1.

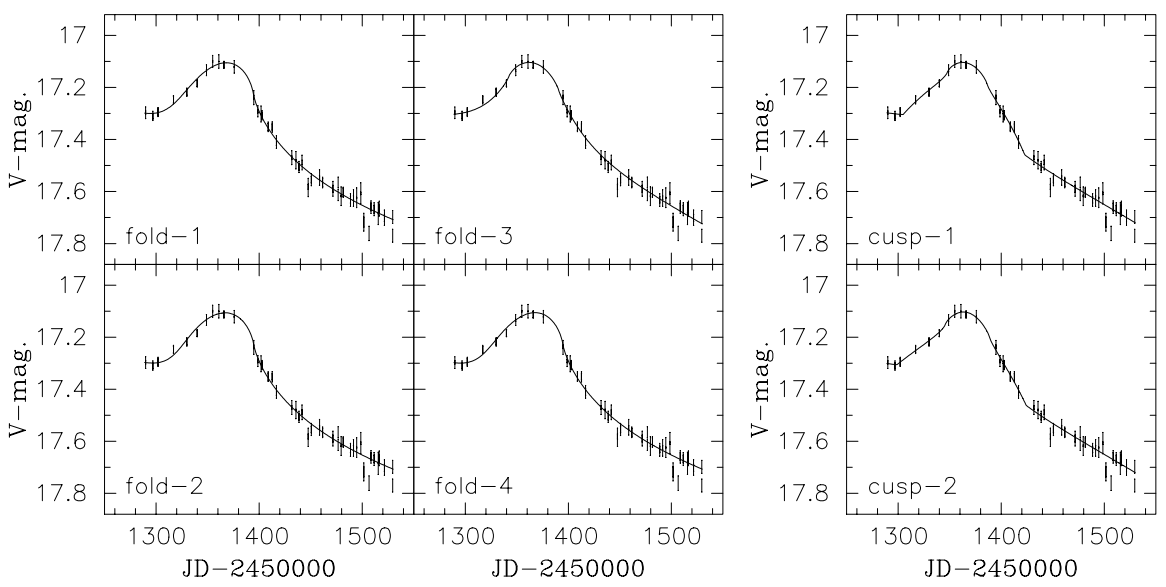

Figure 2 Observational data (bars) and the best-fit light curves (solid lines) in the case of fold caustics (left 4 panels) and in the cause of cusp caustics (right 2 panels).

https://doi.org/10.1071/AS01014 Published online by Cambridge University Press

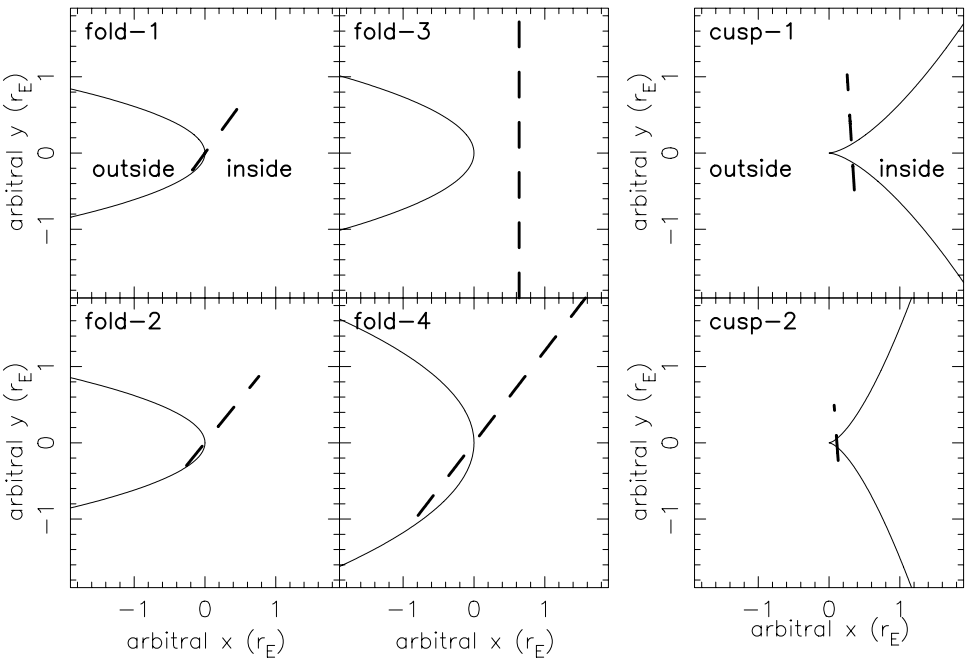

Figure 3 Considered caustics (solid curves) and paths to reproduce the best-fit light curves (dashed lines) are presented.

Table 1. The best-fit source sizes in the unit of the Einstein-Ring radius, 90% confidence regions for the best-fit source sizes obtained by Monte Carlo simulations (see text), and reduced χ^2 values are presented

	fold-1	fold-2	fold-3	fold-4	cusp-1	cusp-2
Size	$0.18^{+0.02}_{-0.02}$	$0.24^{+0.02}_{-0.02}$	$0.85^{+0.13}_{-0.37}$	$0.76^{+0.09}_{-0.07}$	$0.21^{+0.14}_{-0.05}$	$0.10^{+0.08}_{-0.02}$
$\bar{\chi}^2$	1.46	1.49	1.48	1.47	1.33	1.30

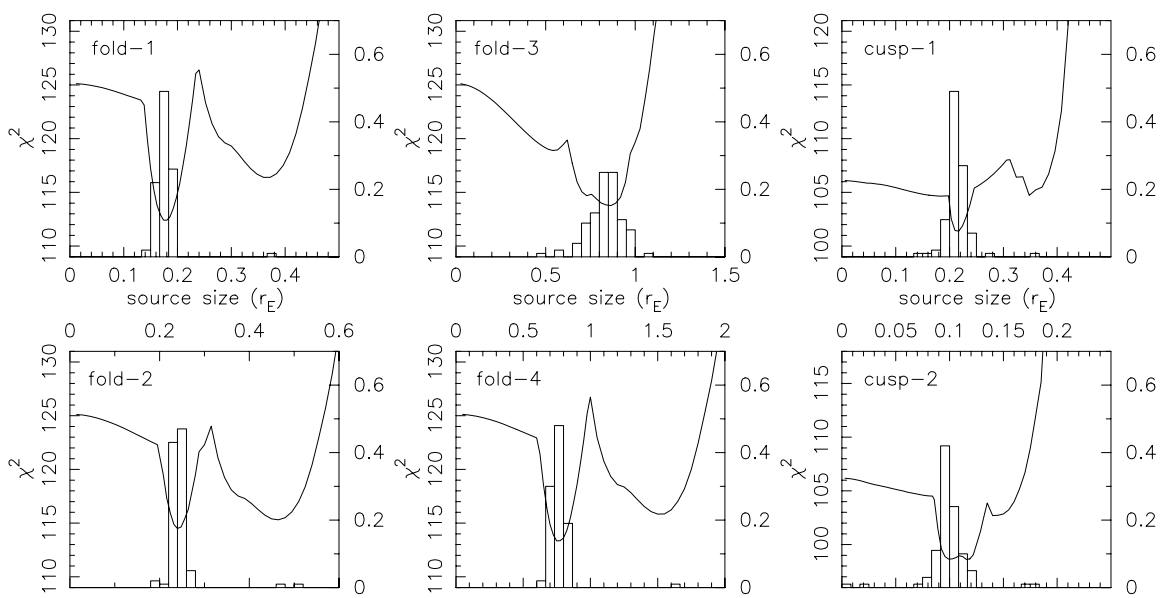

Figure 4 Solid lines show the total χ^2 values between observed light curve and the best-fit light curve for given source sizes. Histograms present the distributions of the best-fit source sizes for mock light curves obtained by Monte Carlo simulations (see text). The unit of source size is the Einstein-Ring radius. Kinks of solid lines are caused by dramatic changes of path of the source to reproduce the best-fit light curve, e.g. from caustics crossing case to caustics grazing case.

https://doi.org/10.1071/AS01014 Published online by Cambridge University Press

For every case, if the source size is larger than the best-fit value, expected magnification will be suppressed too much, the light curve will become shallow, and the fit will not be as good. On the other hand, if the source is smaller than the best-fit value, the expected magnification will be large, the light curve will sharpen, and again the fit will not be as good. These are qualitative reasons why the resultant source sizes are limited in a somewhat small range as presented in Figure 4 clearly. In this figure, not only the total χ^2 values between the observed light curve and the best-fit light curve for given source sizes, but also the distributions of the best-fit source sizes for mock light curves obtained by Monte Carlo simulations are depicted.

There are no clear differences in the goodness of fit between all the considered cases, and I cannot unambiguously choose the best set of parameters. From these results, however, I can put a conservative limit on a source size in the units of $r_{\rm E}$. This upper limit is given in the case of fold-3 and I can say that the source size of Q2237+0305 should be smaller than $\sim 0.98\, r_{\rm E}$ (more than 90% confidence level). Since the Einstein-Ring radius of quasar microlensing is typically $\leq 1\,\mu$arcsec, this result indicates the existence of a sub-μarcsec source in a quasar!

To convert the limit in the units of $r_{\rm E}$ obtained above into physical units I have to calculate $r_{\rm E}$ for relevant parameters. Fortunately, in the case of Q2237+0305, the Einstein-Ring radius weakly depends on cosmological parameters. Assuming the mass of the lens object and Hubble's constant are equal to $1.0{\rm M}_\odot$ and $70\,{\rm km\,s^{-1}\,Mpc^{-1}}$ respectively, the Einstein-Ring radius will correspond to $\sim 10^{17}$ cm and the source size should be smaller than $\sim 10^{17}$ cm. Moreover, for the $\sim 0.1{\rm M}_\odot$ lens object case suggested by Wyithe, Webster & Turner (2000) as a mean lens mass, the upper limit for the source size will be reduced by a factor of $\sqrt{10}$ and become $\sim 2 \times 10^3$ AU!

The result indicates that there is a luminous ($\sim 10^{43}\,{\rm erg\,s^{-1}}$ $\sim 10^{10}{\rm L}_\odot$ without magnification due to the macrolens effect by foreground, lensing galaxy) but compact object in the central region of this quasar. Until now, at least, we have never discovered and/or recognised such a luminous but compact object except for an accretion disk. Therefore, this result strongly supports the existence of an accretion disk in a quasar.

Acknowledgements

The author would like to express his thanks to S. Mineshige for his extensive support, E.L. Turner, J.S.B. Wyithe, K. Ioka, K. Mitsuda, K. Yoshikawa, T. Takeuchi, M. Umemura, A. Burkert, Y. Suto, and an anonymous referee for their helpful comments. The author also acknowledges the OGLE team for making their monitoring data publicly available. This work was supported in part by the Japan Society for the Promotion of Science (9852).

References

Chang, K., & Refsdal, S. 1984, A&A, 132, 168 (erratum 139, 558)
Fluke, C. J., & Webster, R. L. 1999, MNRAS, 302, 68
Mineshige, S., Yonehara, A., & Takahashi, R. 2001, PASA, 18, 186
Press, W. H., Flannery, B. P., Teukolsky, S. A., & Vetterling, W. T. 1992, in Numerical Recipes (2nd ed.; Cambridge: Cambridge University Press)
Schmidt, R., Webster, R. L., & Lewis, G. F. 1998, MNRAS, 295, 488
Shalyapin, V. N. 2001, Ast. L., 27, 150
Wambsganss, J. 1990, in Gravitational Microlensing, Dissertation der Fakultät für Physik der Ludwig-Maximilians-Universität, München
Wambsganss, J. 2001, PASA, 18, 207
Wambsganss, J., Schneider, P., & Pazcyński, B. 1990, ApJ, 358, L33
Wozniak, P. R., Udalski, A., Szymanski, M., Kubiak, M., Pietrzynski, G., Soszynski, I., & Zebrun, K. 2000, ApJ, 540, L65
Wyithe, J. S. B., Webster, R. L., & Turner E. L. 2000, MNRAS, 315, 51
Yonehara, A. 2001, ApJ, 548, L127
Zakharov, A. F. 1995, A&A, 293, 1